Recycling of FRP Wind Blade Waste Material in Concrete

Meiran Abdo
University of Bristol, Bristol Composites Institute
Queen's Building
University Walk
BS8 1TR.
Eleni Toumpanaki, University of Bristol, UK
Andrea Diambra, University of Bristol, UK
Lawrence C. Bank, Georgia Institute of Technology, USA

ABSTRACT

Fibre-reinforced polymer (FRP) composites are increasingly used across various industries. However, there is a need to integrate end-of-life scenarios into design and manufacturing workflows to reduce the high volumes of landfill waste they generate. According to estimates, the UK and Europe will need to decommission around 52,000 tonnes of wind turbine blades annually. With this rise in blade waste, there is a pressing need for effective recycling solutions. This study investigates the effective use of waste fibre-reinforced polymer (FRP) composite materials as discrete reinforcing elements in concrete for civil engineering applications. The needles were derived from a reclaimed wind blade made of glass FRP (GFRP), with a length of 50 mm and an aspect ratio of 8.3. The GFRP needles were added at 5% volumetrically to the coarse natural aggregate on top of the natural aggregates. The results suggest that incorporating GFRP needles into concrete increases both splitting tensile strength and compressive strength while reducing the slump (workability) compared with the control specimens.

Keywords: FRP waste, sustainability, concrete, mechanical characterisation.

INTRODUCTION

The UK net zero strategy has impacted all industries, including construction and energy, requiring the adoption of sustainable practices from design and manufacturing to end-of-life. The civil engineering sector is under increasing pressure to adopt strategies that improve construction systems' mechanical and durability performance while reducing their environmental footprint [1,2]. The renewable energy industry, specifically the wind energy sector, is experiencing unparalleled expansion [3]. High demand presents a challenge for disposing of end-of-life wind turbine blades [4]. These blades mainly consist of fibre-reinforced polymer (FRP) composites, which are difficult to recycle due to the complexity of their material composition and adhesive joints adopted between components [5,6]. The increase in wind turbine blade waste is estimated to exceed ten thousand tons every year globally [7]. Suggested FRP recycling techniques like pyrolysis and solvolysis adopt significant energy and costly methods that require high temperatures and chemicals. Thus, a less environmentally harmful and cost-effective approach is needed to solve this issue. Mechanical recycling and cutting GFRP wind turbine blades into GFRP needles or aggregates for concrete applications offers a promising approach to downcycling and repurposing waste from one industry into an efficient structural material in another sector. Undoubtedly, concrete is considered the primary building material, consuming significant energy and raw materials [8]. Therefore, substituting GFRP waste materials for virgin materials in buildings facilitates the achievement of environmental advantages and contributes to sustainability. A limited investigation has been done by several researchers studying the use of recycled GFRP in concrete materials [9-11]. Besides, some research is related to making FRP rebar into "needles" to replace concrete. Zhou et al. [12] found that the compressive strength decreased as the RGFA replacement ratio increased. At a 30% replacement ratio, the strength decreased by 56.52%. When RGFAs completely replaced the NCAs, the compressive strength of the RFAC specimen was only about one-seventh of the NCA specimen. This study addresses a significant research gap by investigating the effect of GFRP needles as discrete reinforcement elements on tensile and compressive concrete mechanical performance. This set of experiments will inform future studies in optimum GFRP needle geometries and interfacial GFRP needle/concrete properties. In this work, the natural aggregate is referred to as NA, and the cut piece of FRP waste is FRP-DR, which stands for FRP-Discrete Reinforcement.

EXPERIMENTAL PROGRAMME

Materials and Concrete Mixtures

Needles with parallelepiped shapes having 6 mm x 6 mm cross-sections and lengths of 50 mm were produced from reclaimed wind turbine blades provided by Vestas (Isle of Wight). The needle's dimensions were determined following previous work conducted in previous studies. In these studies, the needles had the same cross-section and length of 100mm, while the proposed needles are shorter to be used as an aggerate replacement and short reinforcement; this short length will also allow an easy needle flow when used with reinforcements. The raw material provided consisted of thick GFRP panels with varying thicknesses ranging from 10 mm to 80 mm, as depicted in Figure 1. The exact location of the wind turbine blade is still to be determined. A fundamental limitation of reclaimed materials lies in identifying their mechanical properties. This is due to limited accessibility to proprietary data and the long-term effects of their stress and environmental conditioning history. Key experiments were conducted to gather data about the provided GFRP panels, including fibre content following ASTM D2584 [13], density, and tensile strength based on ASTM D3039M [14], as shown in Table 1. To determine the laminae fibre orientation in the reclaimed GFRP panels, microscopy imaging using Zeiss microscopy and GFRP burn-out tests were used according to ASTM D2584 [13]. The laminate consists of two Quasi-Isotropic +/—45° layers and nine 0° Layers.

Figure 1. End-of-life wind turbine blade.

Table 1: Properties of GFRP reclaimed wind blade.

Properties	Type (Value)
Fibre content by weight of GFRP panel (%)	64
Density (kg/m^3)	1970 ± 4.6
Tensile strength of GFRP panel (MPa)	649.62 ± 7.8
Tensile modulus of elasticity of GFRP panel (GPa)	26 ± 1.7
Fibre type*	E-glass fibre

Notes: 1) *Most GFRP wind turbine blades are made of E-glass fibres [15]. 2) Average values ± Standard deviation.

Crashed limestone was used as aggregate, and a sieve analysis was conducted to ensure it complied with ASTMC33 standards [16]. Type I Portland cement and ASTM-graded sand were used in all concrete mixtures. Both the aggregates and sand were at saturated surface-dry (SSD) conditions to ensure a consistent water/cement ratio. Two concrete batches were prepared: one for the control specimens ('Control-NA') without GFRP needles and another for specimens with 5% GFRP needles ('FRP-DR-5'). Each batch produced eight cylinders with a height of 300 mm and a diameter of 150 mm. Four were used for compressive strength tests, where the compressive modulus of elasticity was measured, and the remaining four were used for splitting tensile strength tests. The concrete mixture properties are presented in Table 2. In the 'FRP-DR-5' specimens, 5% by volume of coarse aggregate was added as GFRP pieces to the concrete mixture. The water/cement ratio target of the concrete mixes was 0.45. A low moisture absorption of the GFRP needles is assumed; therefore, no watercontent adjustment was made. After 24 hours, the concrete samples were de-moulded and put into a water-curing tank for 14 days. This facilitates earlier evaluation of concrete performance, thus enabling potential adjustments in mix design or construction processes. Furthermore, the early strength results obtained can be beneficial in scheduling subsequent construction activities. A slump test was performed according to ASTM C143 [17].

Table 2: Proportions of concrete mixtures for the two concrete batches.

	Mixture	
	Control - NA	FRP-DR-5
Cement (kg/m^3)	422	422
Sand (kg/m^3)	683	683
Aggregate (kg/m^3)	950	902
Water (kg/m^3)	190	190
FRP Needles (no.)	0	76
Slump (mm)	75	63

TEST METHOD

After curing the specimens for 14 days, split tensile and compression strength tests were conducted in both the ‘Control-NA’’ and FRP-DR-5' specimens. The INSTRON 600DX with a maximum load capacity of 600 kN was used for the split tensile test, and the Testwell automatic compression testing machine with a maximum load capacity of 3000 KN was used for the compression strength tests. The concrete compressive strength and the modulus of elasticity (compressive) were evaluated according to ASTM C469[18]. The split tensile strength was calculated according to ASTM C496 [19]. An LVDT set-up was made at the University of Bristol to measure the compressive modulus of elasticity, as shown in Figure 2. One LVDT at each side of the concrete cylinder was used to record relative contraction within a gauge length of 150 mm.

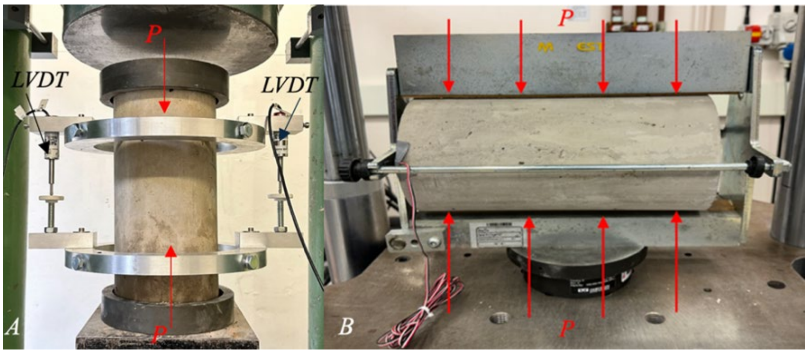

a) Compressive test and LVDT setup b) Split tensile test.

Figure 2. Mechanical characterisation of both ‘Control-NA’ and ‘FRP-DR-5’ concrete specimens.

RESULTS AND DISCUSSION

Slump flow

The 5% volumetric dosage of the GFRP needle addition in the concrete specimens reduced the slump test by 16% compared with the control specimens. This difference is due to the rougher surface of the GFRP needles, higher surface area and increased interlocking between the needles and the concrete mix that impede concrete flowability, as also reported in fibre-reinforced concrete [19]; moisture absorption in FRP needles during mixing is expected to be low. Fibre addition reduces the slump flow measurements in fibre-reinforced concrete, making the mix slightly viscous ACI 544.1[21]. However, the size and aspect ratio of the fibres cannot justify fibre agglomeration as observed in fibre-reinforced concrete [22].

Concrete compression performance

Table 4 presents compressive test results, including strength and elastic modulus values. For compressive tests, 4 specimens per variable have been tested, and a potential outlier has been identified. Due to space limitations in curing tanks, the 'Control- NA-1' specimen was placed in a different curing tank with an uncontrolled temperature. The low temperature caused a slow cement hydration and delayed the concrete strength gain. Another study reported that the compressive strength growth trend indicated a big difference at different temperatures from 7 to 14 days of hydration age [23]. The 5% aggregate volumetric addition of GFRPs in the concrete specimens resulted in a 15% strength increase compared to Control-NA specimens, while the elastic modulus values were reduced by only 1.4%. Conversely, in concrete, there is a typical enhancement of both properties. The increase in compressive strength is typically associated with a higher modulus of elasticity [24]. Other authors have noted that adding a recycled concrete aggregate will deteriorate both properties due to poor adhesion [25]. However, changing the raw materials in concrete will not only influence the compressive strength and modulus of elasticity of concrete but also change how those properties interact [26]. A similar study with a slightly different needle size has shown that concrete compressive strength decreases by 3-6% with a 5-10% GFRP replacement ratio; the needles were generated from waste FRP rebars and cut to 100mm with an aspect ratio of 17 [2]. Nevertheless, the GFRP needles have lower bonding strength than the natural aggregate, which could lead to an ineffective stress transfer, impacting the GFRP needle's elastic response and reducing its elastic modulus.

Table 4: Compressive test results

Concrete Type	Specimen	f_c (MPa)	f_{cm} (MPa)	$f_{cm\sigma}$ (MPa)	E_c (GPa)	E_{cm} (GPa)	$E_{c\sigma}$ (GPa)
Control-NA	2	30.89	35.31	3.4	31.7	33.42	1.29
	3	35.72			33.76		
	4	39.3			34.81		
FRP-DR-5	1	39.37	40.62	0.8	34.45	32.95	1.02
	2	40.51			32.76		
	3	41.73			34.01		
	4	40.88			31.57		

Note: f_c= Compressive strength values, f_{cm}= Mean compressive strength, $f_{cm\sigma}$= standard deviation in compressive strength E_c= compressive elastic modulus values, E_{cm} = Mean compressive modulus, and $E_{c\sigma}$= standard deviation in compressive modulus.

Concrete split tensile performance

Table 5 presents the results from split tensile strength testing. The 5% volumetric addition of the GFRP needles increased the concrete split tensile capacity by 26.9% compared to the control samples. A previous study [11] reported a 32% improvement in concrete tensile properties when incorporating 2.5% GFRP needles as an aggregate replacement to control concrete, using similar needle geometry and aspect ratio. Other authors have also indicated a similar trend of increase in the splitting tensile strength of concrete, replacing 5-10% of natural aggregate with GFRP-Needles. The splitting tensile strength of concrete was increased by 22% and 33%, respectively, in these cases [26]. This is attributed to the high tensile properties of the GFRP needles combined with a sufficient bonded length and GFRP/concrete bond properties that allow a crack-bridging effect.

Table 5: Split tensile strength test results.

Concrete	Specimen	f_{ct} (MPa)	f_{ctm} (MPa)	$f_{ct\sigma}$ (MPa)
Control-NA	5	3.09	2.6	0.4
	6	2.37		
	7	3.5		
	8	2.82		
FRP-DR-5	5	3.64	3.3	0.2
	6	3.03		
	7	3.58		
	8	3.62		

Note: f_{ct} = tensile strength, f_{ctm} = average tensile strength, $f_{ct\sigma}$ = standard deviation tensile test results.

Stress-strain plots

The stress-strain plots for the concrete compressive and tensile tests are shown in Figure 3. Only the upper and lower boundaries among the ‘Control-NA’ and ‘FRP-DR-5’ specimens are considered. Figure 3 (a) shows that ‘Control-NA’ concrete samples crush immediately after reaching the peak compressive load value. ‘FRP-DR-5’ concrete specimens, similar to ’Control-NA’ specimens, also fail immediately in compression after reaching the peak load value. This indicates an unsuccessful crack-bridging and crack arrest effect due to several hypothetical reasons, such as insufficient needle length, which limits the concrete connection across the crack and the ability of needles to hold the concrete together [28]. Another reason can be the weak bonding between the GFRP needles and the concrete. Short needles have less surface area than concrete, which leads to poor stress transfer, which causes the GFRP needles to pull out the matrix instead of failing. Figure 3 (b) shows that ‘FRP-DR-5’concrete exhibits a significantly higher failure strain than Control-NA for tensile testing. During the split tensile tests for ‘Control-NA’, the cylinders were broken and split into two separate pieces sooner after reaching the peak load. On the other hand, ‘FRP-DR-5’ concrete specimens only developed cracks, and they did not collapse into two separate pieces, but they maintained some integrity. The post-tensile strength retention is limited. This can be attributed to the nature of the split tensile test, which does not allow activation of the crack bridging effect compared to a bending test. These results support the findings in [9] that the needles are more effective in splitting tensile rather than compressive testing conditions.

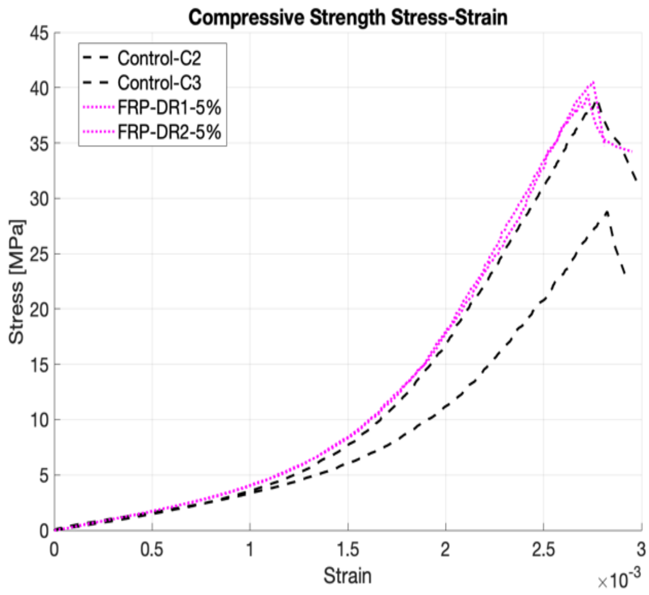

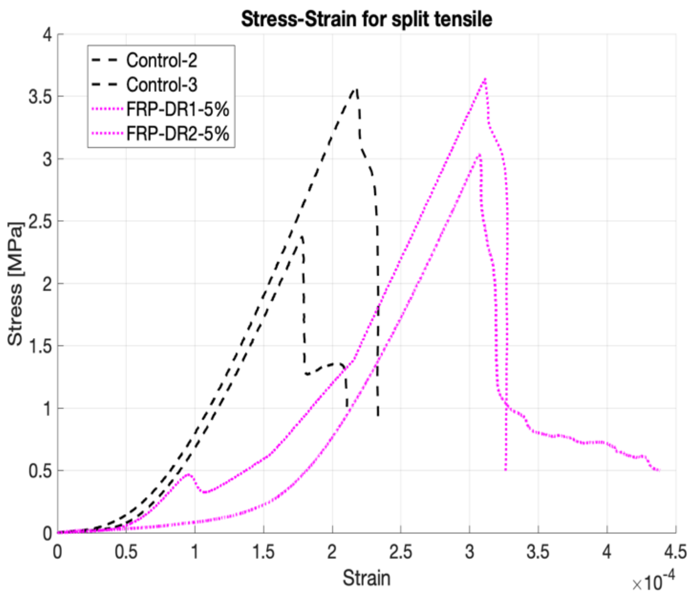

a) Compressive testing b) Split tensile test.

Figure 3. The stress-strain relationship plots for both control and GFRP reinforced concrete.

CONCLUSIONS

This work presented the use of GFRP needles with a small aspect ratio as discrete reinforcement in concrete. The results suggest that adding GFRP needles can positively affect compressive and split tensile strength.

- The addition of 5% GFRP needles improved compressive strength and split tensile strength by 15% and 26.9%, respectively, compared with the ‘Control-NA.’
- The addition of GFRP needles was more effective in splitting-tensile rather than compression testing conditions.
- The workability of the concrete reduced the slump test by 16% compared with the control specimens.

REFERENCES

1. Guerra BC, Shahi S, Mollaei A, Skaf N, Weber O, Leite F, et al. Circular economy applications in the construction industry: A global scan of trends and opportunities. Journal of Cleaner Production [Internet]. 2021;324:129125.
2. Sizirici B, Fseha Y, Cho CS, Yildiz I, Byon YJ. A Review of Carbon Footprint Reduction in Construction Industry, from Design to Operation. Materials. 2021 Oct 15;14(20):6094.
3. Energy Agency I. Renewables 2020 - Analysis and forecast to 2025.
4. WWEA. World wind capacity at 650,8 GW, Corona crisis will slow down markets in 2020, renewables to be core of economic stimulus programmes. 2021.
5. Yang Y, Boom R, Irion B, van Heerden DJ, Kuiper P, de Wit H. Recycling of composite materials. Chemical Engineering and Processing: Process Intensification [Internet]. 2012;51:53–68.
6. Belarbi A, Dawood M. Sustainability of fiber-reinforced polymers (FRPs) as a construction material. In 2016. p.521–38.
7. Qureshi J. A Review of Recycling Methods for Fibre Reinforced Polymer Composites. Sustainability [Internet]. 2022;14(24).
8. Sandanayake, M.; Zhang, G.; Setunge, S. Estimation of environmental emissions and impacts of building construction—A decision making tool for contractors. J. Build. Eng. 2018.
9. Yazdanbakhsh A, C. Bank L, Chen C. Use of recycled FRP reinforcing bar in concrete as coarse aggregate and its impact on the mechanical properties of concrete. Construction and Building Materials [Internet]. 2016;121:278–84.
10. Zhao T, Lv Y, Chen J, Song P, Sun M, Zhang X, et al. Effect of Glass Fiber-Reinforced Plastic Waste on the Mechanical Properties of Concrete and Evaluation of Its Feasibility for Reuse in Concrete Applications. Materials [Internet]. 2023;16(20).
11. Abdo M, Toumpanaki E, Diambra A, Bank LC. Evaluation of mechanical properties of concrete with recycled FRP wind blade waste material.
12. Zhou Y, Weng Y, Li L, Hu B, Huang X, Zhu Z. Recycled GFRP Aggregate Concrete Considering Aggregate Grading: Compressive Behavior and Stress-Strain Modeling. Polymers (Basel). 2022 Jan 31;14(3):581. doi: 10.3390/polym14030581. PMID: 35160571; PMCID: PMC8839721.
13. ASTM. "Standard Test Method for Ignition Loss of Cured Reinforced Resins", ASTM D2584. (2018).
14. ASTM."Standard Test Method for Tensile Properties of Polymer Matrix Composite Materials." ASTM D3039. (2017).
15. Eker B, Akdoğan Eker A, Vardar A. Using of Composite Material in Wind Turbine Blades. Journal of Applied Sciences. 2006 Apr;6.
16. ASTM. "Standard specification for concrete aggregates." ASTM C33, West Conshohocken, PA. (2013).
17. ASTM. "Standard Test Method for Slump of Hydraulic-Cement Concrete." ASTM C143. (2015).
18. ASTM. "Standard test method for static modulus of elasticity and Poisson's ratio of concrete in compression." ASTM C469, West Conshohocken, PA. (2014).
19. ASTM. "Standard test method for splitting tensile strength of cylindrical concrete specimens." ASTM C496, West Conshohocken, PA. (2011).
20. Ahmad J, González-Lezcano RA, Majdi A, Ben Kahla N, Deifalla AF, El-Shorbagy MA. Glass Fibers Reinforced Concrete: Overview on Mechanical, Durability and Microstructure Analysis. Materials (Basel). 2022 Jul 22;15(15):5111. doi: 10.3390/ma15155111.
21. ACI (American Concrete Institute). (2009). "Report on fiber reinforced concrete, 544.1 R-96 (reapproved 2009)." ACI 544.1, Farmington Hills, MI.
22. Bentur, A., and Mindess, S. Fiber reinforced cementitious composites, Taylor & Francis, New York. (2007).
23. Liu, J., Li, Y., Yang, Y., Cui, Y,. Effect of low temperature on hydration performance of the complex binder of silica fume-Portland cement. J. Wuhan Univ. Technol.-Mat. Sci. Edit. 29, 75–81 (2014).
24. Revilla-Cuesta, V.; Fiol, F.; Perumal, P.; Ortega-López, V.; Manso, J.M. Using recycled aggregate concrete at a precast-concrete plant: A multi-criteria company-oriented feasibility study. *J. Clean. Prod.* 2022, *373*, 133873.
25. Silva, R.V.; De Brito, J.; Dhir, R.K. The influence of the use of recycled aggregates on the compressive strength of concrete: A review. *Eur. J. Environ. Civ. Eng.* 2015, *19*, 825–849.
26. Revilla-Cuesta, V.; Faleschini, F.; Pellegrino, C.; Skaf, M.; Ortega-López, V. Simultaneous addition of slag binder, recycled concrete aggregate and sustainable powders to self-compacting concrete: A synergistic mechanical-property approach. *J. Mater. Res. Technol.* 2022, *18*, 1886–1908.
27. Yazdanbakhsh A., Bank L.C., Chen C., Tian Y. FRP-needles as discrete reinforcement in concrete. J. Mater. Civ. Eng. 2017;29:04017175. doi: 10.1061/(ASCE)MT.1943-5533.0002033.
28. ASTM. " Standard Test Method for Flexural Performance of Fiber-Reinforced Concrete Using Beam With Third-Point Loading". ASTM C1609. (2010).